DMD Fast Forward. Published on March 19, 2007 as doi:10.1124/dmd.106.013250

DMD#13250

Structure-Activity Relationships for Interaction with Multidrug Resistance Protein 2 (ABCC2/MRP2): The Role of Torsion Angle for a Series of Biphenyl-Substituted Heterocycles

Yurong Lai*, Li Xing, Gennadiy I Poda, Yiding Hu

Pfizer, Inc. St Louis Laboratory, 700 Chesterfield Parkway West, Chesterfield, MO 63017

RUNNING TITLE PAGE

a) Running title: SAR of ABCC2/MRP2 interactions for the biphenyl-substituted heterocycles

b) Corresponding author:

Dr. Yurong Lai,

Pharmacokinetic, Dynamics, & Metabolism, Pfizer, Inc. St Louis Laboratory,

700 Chesterfield Parkway West, Chesterfield, MO 63017.

Tel: 314-274-5908 Fax: 314-274-4426

Email: yurong.lai@pfizer.com

c) Number of text pages:

Number of tables: 2
Number of Figures: 5
Number of references: 52
Number of words in Abstract: 245
Number of words in Introduction: 402
Number of words in Discussion: 2709 (results and discussion)

d) Abbreviations: SAR, Structure-activity relationship; MK571, [3-[[3-[2-(7-chloroquinolin-2-yl)vinyl]phenyl]-(2-dimethylcarbamoylethylsulfanyl)methylsulfanyl] propionic acid]; ABCC2/MRP2, Multidrug resistance protein 2; Caco-2, human colon carcinoma cell.

Abstract:

Multidrug resistance protein 2 (ABCC2/MRP2) is an ATP-binding cassette transporter involved in the absorption, distribution and excretion of drugs and xenobiotics. Identifying compounds that are ABCC2/MRP2 substrates and/or inhibitors and understanding their structure-activity-relationships (SAR) are important considerations in the selection and optimization of drug candidates. In the present study, the interactions between ABCC2/MRP2 and a series of biphenyl-substituted heterocycles were evaluated using Caco-2 cells and human ABCC2/MRP2 gene transfected MDCK cells. It was observed that ABCC2/MRP2 transport and/or inhibition profile, both in nature and in magnitude, depends strongly on the substitution patterns of the biphenyl system. In particular, different ortho-substitutions cause various degrees of twisting between the two-phenyl rings, resulting in changing interactions between the ligands and ABCC2/MRP2. The compounds with small ortho functions (hydrogen, fluorine and oxygen), thus displaying the smallest torsion angles of biphenyl (37^o – 45^o), are neither substrates nor inhibitors of human ABCC2/MRP2. The transporter interactions increase as the steric bulkness of the ortho-substitutions increase. When the tested compounds are 2-methyl substituted biphenyls, they exhibit moderate torsion angles (54^o -65^o) and behave as ABCC2/MRP2 substrates as well as mild inhibitors (10-40% compared to MK571). For the 2, 2'-dimethyl substituted biphenyls, the torsions are enhanced (78^o – 87^o), and so are the inhibition of ABCC2/MRP2. This class of compounds behaves as strong inhibitors of ABCC2/MRP2. These results can be used to define the three-dimensional structural requirements of ABCC2/MRP2 interaction with their substrates and inhibitors, as well as provide SAR guidance to support drug discovery.

Multidrug resistance-associated protein (MRP), currently consisting of nine members (MRP1-9, also named ABCC1-6, ABCC10-12), is one branch of the ATP-binding cassette (ABC) superfamily of transmembrane proteins that use the energy of ATP-hydrolysis to translocate their substrates across biological membranes (Borst et al., 2000; Kruh and Belinsky, 2003; Schinkel and Jonker, 2003). ABCC2/MRP2 is mainly expressed in the apical membrane of liver canaliculi, renal proximal tubules, gut enterocytes, placenta and brain-blood barrier. The substrates of ABCC2/MRP2 include non-conjugated amphipathic organic anions and glucuronide, glutathione, and sulfate conjugates (Suzuki and Sugiyama, 1998; Keppler and Konig, 2000). ABCC2/MRP2 also transports various unmodified drugs including vincristine (Keppler et al., 2000), doxorubicin (Koike et al., 1996; Cui et al., 1999), HIV protease inhibitors (Gutmann et al., 1999), nucleoside phosphonates (Miller et al., 2001), p-aminohippuric acid (Leier et al., 2000) and fluoroquinolone antibiotics (Naruhashi et al., 2002). Therefore, ABCC2/MRP2, being a primary active efflux transporter, is functionally similar to P-glycoprotein as both are involved in the hepatobiliary elimination and intestinal absorption of many structurally diverse xenobiotics and their conjugates (Cui et al., 1999; Kusuhara and Sugiyama, 2002). The physiological, pharmacological and clinical implications of ABCC2/MRP2 have been shown on the reviews (Fardel et al., 2005; Robertson and Rankin, 2006).

It is of great value to establish structure-activity relationships (SAR) for ABCC2/MRP2 during the lead optimization stage of drug discovery. For example, researchers have been attempting to elucidate SAR on potent MRP1 inhibitors for cancer chemotherapy (Wang et al., 2004; van Zanden et al., 2005). Two types of molecules have been identified as MRP1 inhibitors or

substrates based on their transport mechanism: a) compounds co-transported with glutathione (GSH) and cytosolic glutathione S-transferases (GST) and (b): compounds interacting with MRP independently from GSH and GST. For compounds that co-transport with GSH and GST their transporter interactions are poorly understood. In contrast, for the GSH/GST independent compounds certain structural requirements have been drawn (Boumendjel et al., 2005). For example, aromatic / heteroaromatic moieties, nitrogen atom and carbonyl groups are frequently observed as MRP1 inhibitors / substrates. However, most of these reports are scattered observations rather than in-depth SAR investigations on MRP(s). In this study, we have carefully selected a group of biphenyl-substituted heterocycles and evaluated their transport and inhibition properties in Caco-2 cells and gene transfected MDCK cells. Based on the analysis we were able to derive a structure-activity relationship for this class of congeneric compounds and infer the structural requirements of ABCC2/MRP2 interactions.

Materials and Methods:

Compounds and reagents:

Dulbecco's Modified Eagle Medium (DMEM), minimum essential medium (MEM), fetal bovine serum (FBS), non-essential amino acids, Glutamax, sodium pyruvate, gentamicin, L-glutamine and Hank's balanced salt solution (HBSS) were purchased from Gibco (Carlsbad, CA). MK571 was obtained from BioMol (Plymouth Meeting, PA). Calcein acetoxymethyl ester (Calcein-AM) was obtained from Molecular Probes (Eugene, OR). Verapamil and novobiocin were purchased from Sigma-Aldrich (St. Louis, MO).

Cell culture

Caco-2 cells (ATCC, VA) were maintained in DMEM with 10% FBS, 1% Non-essential amino acids, 1% Glutamax, 1 mM Sodium Pyruvate and 0.06 mg/ml Gentamicin. Parental Madin-Darby Canine Kidney (MDCK) cells and MDCK cells stable expressing human ABCC2/MRP2 cDNA (MDCK-MRP2; Dr. P. Borst, The Netherlands Cancer Institute, Amsterdam, The Netherlands), were cultured in MEM with L-glutamine containing 10% FBS, 100 unit penicillin and 100 μg/ml streptomycin. Both MDCK and Caco-2 cells were incubated at 37^{o}C in 95% air/ 5% CO_2 with 95% humidity. Cell culture media was refreshed at 3 days interval.

Transcellular transport across Caco-2 cell monolayers and Michaelis-Menten Constant

Caco-2 cells were seeded at a density of 1x10^5 cells/cm^2 onto Millipore 24-well insert plates (Millipore, NJ) and cultured for 21-25 days. Transepithelial electrical resistance (TEER)

values were measured to ensure that tight junctions are formed ($\geq$ 600 Ohm/cm^2, millicell-ERS; Millipore, MA). After washing the transwell filter with HBSS (pH 7.4), each compound was applied to the donor side (either apical or basal chamber) at a concentration of 10 μM to initiate the transport assay. The transport incubation was maintained at 37˚C for 2 hrs on a shaking incubator (Precision Scientific, VA). Aliquots (200-μl) were collected from both the apical and basal sides, and compound concentrations were determined by LC/MS/MS. The extent of permeation (P_{app}) was generated for both A→B and B→A transport. The efflux ratio was calculated from ($P_{app, B\rightarrow A}$)/($P_{app, A\rightarrow B}$). An efflux ratio ≥2 indicates that transport is apically polarized (active efflux). The compounds actively effluxed by Caco-2 cells were further applied to the Caco-2 transport assay in the presence of 25 μM MK571 to assess transport under conditions of ABCC2/MRP2 specific inhibition. For the measurement of concentration dependent transport in Caco-2 cells, the compounds (0.5-50 μM) were added to initiate transport, and an aliquot (200 μl) of the incubation buffer in the receiver chamber was collected at 120 min. The active efflux rate (B to A transport) was determined from the appearance of the compounds in the receiver compartment over the time period. Several models were fitted using nonlinear regression (WinNonlin; Pharsight Corporation, Mountain View, CA) to analyze the transport curves. The best fit model was identified based on the reduction in the sum of squared residuals and Akaike's Information Criterion (AIC).

Inhibition of calcein efflux mediated by ABCC2/MRP2

MDCK-MRP2 cells were grown on a 96-well cell culture plate for 4 to 5 days and allowed to become confluent. After being washed twice with HBSS buffer, the cells were pre-incubated

with 100 µl of test compound (80 µM) or MK571 (25 µM) in HBSS containing 1% DMSO at 37°C for 15 min. Calcein-AM was then added into the well to yield a final concentration of 1 µM for 20 mins. To minimize the calcein-AM efflux by P-gp or ABCC2/MRP2 during the loading phase, calcein-AM loading was conducted on ice. The cells were quickly washed twice with cold HBSS buffer and replaced with 100 µl of the test compound (80 µM) or MK571 (25 µM) for 1 hr at 37°C. The cells were quickly washed twice with ice cold HBSS buffer, and then lysed by 1% Triton with 0.01% antifoam. The cell lysate was transferred to a 96-well clear bottom assay plate (Corning, NY), and the fluorescent intensity of calcein was measured using a fluorescent spectrophotometer with an excitation wavelength of 485 nm and an emission wavelength of 530 nm. Quantification of ABCC2/MRP2 inhibition was completed using the following equation: % maximum = $(FU_{comp}-FU_{backgroup})/(FU_{MK571}-FU_{backgroup})*100$; where FU_{comp} is the fluorescence value in the presence of test compound and FU_{MK571} is the fluorescence value in the presence of 25 µM MK571.

The structure and physicochemical parameters of biphenyl compounds

A series of biphenyl substituted heterocyclic compounds was selected from archive storage at Pfizer Global Research and Development (St. Louis Laboratories, St. Louis, MO) based on similarity of substructure definitions. This 4-heterocyclic moiety contains a pyrazole with two branched polar functional groups: 3-carbamoyl and 4-urea (Table 1). The only structural variation among the selected compounds is located on biphenyl rings substituted with a variety of atoms or functional groups at 2-, 2'-, 3-, and 3'- positions. The substituting groups include halogens (F, Cl, Br), methyl, trifluoromethyl, hydroxy, methoxy and ethoxy, which differentiate the physicochemical properties and the three-dimensional conformations of each

individual compound. The physicochemical properties, characterizing the overall lipophilic and electronic properties of the test compounds, were calculated using *in silico* methods from an internally produced computational package. These included ClogP, hydrogen bond donor and acceptor counts and topological polar surface area (tPSA).

Measurement of distribution coefficient of compounds (LogD):

LogD measurements were conducted by equilibrating compounds in octanol saturated with 50 mM sodium phosphate buffer (pH 7.4) of ionic strength (0.15 M) for 72 hrs at ambient temperature. The fraction of the drug in each layer was measured by HPLC using diode array detection. LogD at pH 7.4 was calculated by the equation:

$$\text{Log D} = \log \frac{[\text{Area counts of the drug in octanol layer}]}{[\text{Area counts of the drug in aqueous layer}]}$$

Methods for molecular modeling

In recognition of ABCC2/MRP2 interactions, the three-dimensional structure of the ligand is considered to be an important parameter. Specifically, for the compounds under investigation, the torsion angles between the two phenyl groups appear to be extremely sensitive to the different *ortho* substitutions (2, 2- and 2', 2'- substitution). Initial three-dimensional conformers were generated *via* a 2D-to-3D conversion algorithm CONCORD (Tripos, Inc., St. Louis, MO). The conformers were then submitted to full energy minimizations by *ab initio* calculations using the Gaussian98 program (Revision A.11, Gaussian Inc., Pittsburgh, PA). We used a basis set 6-31G*, and a Density Functional Theory (DFT) treatment with Becke potential, B3LYP/6-31G*. To avoid convergence problems the structures were pre-minimized

at STO-3G level for 100 cycles prior to DFT calculations. A default convergence criterion was used.

To understand the importance of molecular fields around the molecules in their interaction with ABCC2/MRP2, Comparative Molecular Field Analysis (CoMFA) was applied to calculate the minimum energy conformers using Sybyl 7.0 (Tripos, Inc. St. Louis, MO). The GASTEIGER method was used to calculate the atomic partial charges. The molecules are aligned by their cogeneric core, the amide urea pyrazole moiety specifically. After the alignment, the molecules were placed in a three-dimensional cubic lattice with 2 Å spacing. The steric (van der Waals) and electrostatic (Coulombic) fields were calculated for each molecule at each mesh point using a sp^3 carbon probe with +1.0 charge. Any calculated steric and electrostatic energies that were greater than 30 kcal/mol were truncated to this value.

HPLC/MS/MS analysis:

The HPLC-MS system consisted of a Hewlett-Packard (HP) 1100 quaternary pump with membrane degasser (Hewlett Packard, Palo Alto, CA), a LEAP CTC Pal liquid handler (SpetraLab Scientific Inc, Toronto, Ontario, Canada) and a PE Sciex API 2000 mass spectrometer (Applied Biosystems, Foster City, CA). A 10 µl sample was injected onto a C18 HPLC column (BetaMax Neutral 20x2.1 mm, Thermo, CA) and eluted by a mobile phase composed of 90% solvent A (95% H2O/5%ACN with 0.1% Formic Acid) and 10% solvent B (5% H_2O/ 95%ACN with 0.1% Formic Acid). The peak areas of all the analytes and internal standard were quantitated using Analyst 1.4 (MDS SCIEX, Ontario, Canada).

Data analysis:

Data are expressed as mean ± SD of transport values obtained in three wells or filter inserts. Data are representative of the minimum of two experiments carried out on different days on different batches of cells.

Results and Discussion

ABCC2/MRP2 mediated transport in Caco-2 monolayer and structures of test compounds

Caco-2 cell monolayers grown on polycarbonate filters have been reported to express transporters that mimic the human intestinal epithelia cells (Taipalensuu et al., 2001). This cell line has been widely used as an *in vitro* model to elucidate the pathways by which drugs permeate the intestinal mucosa, as well as the structure-transport relationship for efflux transporters (Walle et al., 1999; Artursson et al., 2001; Engman et al., 2001). In this study, a series of substituted biphenyl heterocyclic compounds were selected to investigate their interactions with ABCC2/MRP2 transporter. As indicated in Table 1, the differences between the test compounds lie in their biphenyl portion, specifically the varying substitution groups at the 2-, 2'-, 3-, and 3'- positions of the biphenyl rings. In total twenty-six compounds were included in our investigation, which covered a broad spectrum of mono- and di- substitution patterns including halogens (F, Cl, Br), methyl, trifluoromethyl, hydroxy, methoxy and ethoxy groups. Their chemical structures and IUPAC names for the biphenyl substitution were provided in Table 1.

First, we evaluated the polarized transport of the compounds in Caco-2 cell monolayers to examine the involvement of efflux transporters. Twelve of the twenty-six compounds were effluxed by Caco-2 monolayers with the ratio of permeability B to A versus A to B from 8 to 50 [Table 1]. The efflux by Caco-2 monolayers was offset by adding 25 μM MK571, an MRP antagonist and specific inhibitor [Table 1]. However, neither Verapamil (100 μM) nor

Novobiocin (100 μM), the P-gp or BCRP inhibitor (Gao et al., 2001; Yang et al., 2003; Shiozawa et al., 2004), were able to significantly alter the polarized transport by Caco-2 monolayer cells (Data not shown). These results suggested that the polarized transport of this class of compounds in Caco-2 cells was mediated, at least in part, by multidrug resistance proteins (MRPs). To minimize the potential effects of other efflux transporters, the transport experiments were also conducted in MDCK-MRP2 cells. However, the observed polarized transport in Caco-2 cells was not evident in MDCK-MRP2 monolayers, possibly because of the poor (~3 $x10^{-6}$ cm/Sec) apparent permeability for this set of compounds (data not shown). These results were not unexpected, but rather consistent with the published report that it was difficult to demonstrate the vectorial transport of ABCC2/MRP2 substrates due to their poor penetration across the basolateral membrane (Evers et al., 1998; Sasaki et al., 2002). Therefore, in consideration of the technical involvement of accessing the double transfected MDCK cell lines, we regarded the Caco-2 cell line as a valuable tool for investigating the transport and inhibition properties of our test compounds. Similar application of Caco-2 cells has been reported by Letschert and Matsushima (Letschert et al., 2005; Matsushima et al., 2005). In fact, the mRNA of multidrug resistance-associated protein (MRP) isoforms 1 through 6 (ABCC1-6) have been detected in the human intestine and Caco-2 cells (Prime-Chapman et al., 2004). More specifically, the ABCC2/MRP2 and ABCC3/MRP3 isoforms are expressed extensively in Caco-2 cells while ABCC1/MRP1 and ABCC5/MRP5 expression is minimum (Hirohashi et al., 2000). Different isoforms are also differentiated by their selective expressions on disparate phases of the cell membrane. For example, ABCC2/MRP2 and ABCC3/MRP3 are respectively expressed on brush-border and basolateral membranes in Caco-2 cells (Rost et al.,

2002). Therefore the differential pharmacological sensitivity of apical efflux could provide a tool for dissecting the functional roles of the MRP isoforms.

Due to the specific localization of the MRP family it is expected that ABCC2/MRP2 is the only MRP isoform involved in transport of biphenyl compounds under study in Caco-2 cells. Unlike P-glycoprotein which interacts with hydrophobic drugs, ABCC2/MRP2 protein transports hydrophilic molecules with or without acidic conjugates, such as GSH conjugates (Leier et al., 1996; Rappa et al., 1997). As an organic anion transporter, the ABCC/MRP family actively transports a broad range of substrates including glutathione-S-conjugates, glucoronide conjugates, bilirubin, organic anions and conjugated drugs or their metabolites (Jedlitschky et al., 1997; Madon et al., 1997). However, conjugates or compounds with GSH-dependent transport are difficult to draw structure-activity relationship with ABCC/MRP (Boumendjel et al., 2005). In the current study, Caco-2 monolayer assays were performed under such conditions to suppress the formation of co-transport of glutathione or other conjugates by ABCC2/MRP2. SAR on ABCC2/MRP2 and biphenyl compound interaction was elucidated from the variation of the substituted group on the biphenyl ring with altered physicochemical properties and three-dimension structure.

Correlation between physicochemical properties of biphenyl-substituted heterocycles and efflux or inhibition of ABCC2/MRP2.

Like many ABC transporters, ABCC2/MRP2 can be functionally inhibited by a wide range of structurally and pharmacologically unrelated compounds (Payen et al., 2000; Asakura et al., 2004). Substrate inhibition has also been observed for ABCC2/MRP2 (Sugie et al., 2004). To

investigate the inhibitory profile of ABCC2/MRP2 mediated efflux, an inhibition study was performed in MDCK-MRP2 cells. The inhibition of ABCC2/MRP2 activity was achieved by using calcein as a model substrate. Non-fluorescent Calcein-AM is a lipophilic, highly cell-permeable ester and a substrate for both P-gp and ABCC2/MRP2. The ester bond is rapidly cleaved by intracellular non-specific esterases, generating highly fluorescent calcein, a specific ABCC2/MRP2 substrate with poor cell permeability (Legrand et al., 1998). The inhibition of calcein efflux was measured in the absence or presence of selected biphenyl compounds (80 μM) or MK571 (an ABCC2/MRP2 inhibitor, 25 μM). Compound inhibition of ABCC2/MRP2 was compared to and quantified by MK571 inhibition.

In general, for the compounds that were not effluxed by the Caco-2 monolayers we observed no inhibition of the ABCC2/MRP2 mediated calcein efflux. In contrast, the compounds effluxed by the Caco-2 monolayers also demonstrated inhibition of MRP2 mediated calcein efflux, ranging from weak to strong inhibition (10% to over 100%) when compared to MK571 [Fig. 1]. These results reveal that compounds being effluxed in Caco-2 cells were also capable of inhibiting ABCC2/MRP2 mediated efflux in MDCK-MRP2 cells, which suggests overlapping interactions between substrate and inhibitor binding to the ABCC2/MRP2 protein.

Several authors reported application of the CoMFA approach to understand the importance of molecular fields around the molecules in their interaction with ABCC2/MRP2. Likewise, Nakagome et al. reported that ligand recognition of cMOAT/MRP2 is achieved through interactions in two hydrophobic sites and two electrostatically positive and/or hydrogen bonding acceptor sites (Nakagome et al., 2003). Hirono et al. reported a similar model where

interaction between the ligands and MRP2 occurs in two hydrophobic and two electrostatically positive primary binding sites (Hirono et al., 2005). CoMFA studies have been successfully applied to predict activity of compounds that inhibit the multidrug transporter P-glycoprotein for a series of anthranilamide derivatives (Labrie et al., 2006), 2,4,5- and 2,3,4,5-substituted imidazoles (Kim, 2001), natural and synthetic coumarines (Raad et al., 2006) and tariquadar analogs (Globisch et al., 2006). We attempted to apply the CoMFA approach to our dataset but were not able to build a statistically significant model (q^2=0.30 using 6 components for 26 compounds). Therefore, CoMFA, albeit being a complex algorithm proven to be useful in elucidating protein-ligand interactions of many biological systems, was not able to reveal structural features sensible to the transport properties we discovered for this set of compounds.

The physicochemical properties, including hydrophobicity, hydrogen-bond donors, hydrogen-bond acceptors and polar groups, are common factors considered when evaluating the interactions between transporter and small molecule (Hirono et al., 2005; van Zanden et al., 2005). A simple model has been reported that relates the Wiener's topological index and MRP1 inhibitory activity (Lather and Madan, 2005). The accuracy of prediction of such a model was found to be 88%. The Wiener's topological index is proportional to the size of the molecular graph, a property that reflects the size of the molecule. In our analysis we used molecular weight as a parameter that describes molecular size but did not find any significant correlation with the MRP2-related activities. Furthermore, some structural elements for ABCC1/MRP1 have also been summarized. For example, aromatic or heteroaromatic moieties and carbonyl group are frequently observed (Boumendjel et al., 2005). Due to the overlap of

substrates and/or inhibitors between MRP1 and MRP2 it is assumed that the SAR for ABCC2/MRP2 could follow principles similar to ABCC1/MRP1 (Wang and Johnson, 2003).

In the current study, we attempt to account for the physiochemical properties and three-dimensional steric and electrostatic effects, and investigate their relationship with the ABCC2/MRP2 interactions. For such purposes, the physicochemical parameters for this group of biphenyl substituted heterocycles, including ClogP, the number of hydrogen bond donors, the number of hydrogen bond acceptors and the topological polar surface area (tPSA), were evaluated and correlated to ABCC2/MRP2 transport and inhibition. In addition to calculated properties, LogD values were measured to add one more dimension to the property pool to characterize the lipid-water distribution of the compounds under physiological pH. In general, for the tested biphenyl-substituted heterocycles with a variety of substituting groups on the biphenyl ring, ClogP ranged from 0.89 to 3.37, LogD (pH 7.4) ranged from 0.66 to 3.79, the number of hydrogen bond donors ranged from 5 to 7, the number of hydrogen bond acceptors ranged from 4 to 5, and the tPSA ranged from 125 to 156. While most of the properties fell into the normal range for desirable ADME properties (Lipinski et al., 2001), the tPSA appeared too high for passive transcellular absorption (Palm et al., 1997). Interestingly this is in keeping with the reduced transport in MDCK-MRP2 monolayers compared to the Caco-2 cells we have observed, which also suggested poor permeability for this class of compounds.

To our surprise, no correlations were found between the physicochemical descriptors (ClogP, LogD, hydrogen bond donor/acceptor, tPSA) and the ABCC2/MRP2 efflux in Caco-2 monolayers (substrate) [Fig. 1] or the inhibition of calcein efflux in MDCK-MRP2 cell

(inhibitor) [Fig 2]. This implied that the nature and the strength of the interactions between ABCC2/MRP2 and this class of compounds were not determined by any overall molecular properties, but possibly by certain other parameters that are more specific to the three-dimension conformation of the molecules.

Correlation between three-dimensional molecular conformations and the efflux/inhibition properties of ABCC2/MRP2

In the preliminary studies, it was observed that the inhibition of the ABCC2/MRP2 transporter by biphenyl-substituted heterocycles is sensitive to the substitution patterns at the 2- or 2'-(ortho-) positions. Further structure-activity analysis suggested that the inhibition or transport properties mediated by ABCC2/MRP2 is highly sensitive to the bulkiness of the ortho-substituents on the biphenyl ring system. It was suspected that the increase in bulkiness of the 2- or 2'- substitutions resulted in increased torsion angles between the two phenyl rings, and the conformational change was recognized by ABCC2/MRP2 in a favorable manner leading to the strengthened three-dimensional interaction between the transporter and the test compounds. The three-dimensional molecular conformations, derived from electrostatic interactions and steric repulsions between the ortho-substitutions, seems to be the determining factor for ABCC2/MRP2 recognition and interaction.

To validate this hypothesis, we conducted high level *ab initio* calculations during which the global energy minimum was sought and the geometries of the test compounds were fully optimized. As shown in Figure 3, it was found that for the biphenyl ring system in the

aforementioned scaffold, the torsion angles increased upon increasing bulkiness of the ortho-substituents in the following order: H < F < OH < Cl < Me [Fig 3]. The change in torsional space is largely due to the steric repulsion between the two ortho- substituents from the opposing phenyl rings. While the torsion of the plain biphenyl tends to be skewed to possibly maximize the pi-conjugation, the bulky ortho- substituents force the biphenyl into more orthogonal conformations as we have seen here.

Both the efflux in Caco-2 monolayer and the inhibition of calcein efflux in the MDCK gene transfected cells increased consistently with the increasing torsion angles [Fig 4]. Based on the range of torsion angles, the compounds were classified into three groups, with average torsions at 40, 56 and 84 degrees, respectively. Group I compounds are not effluxed in Caco-2 monolayers, neither are they ABCC2/MRP2 inhibitors. Group II and III compounds are ABCC2/MRP2 substrates with MK571 inhibitable efflux in Caco-2 cells. Furthermore, while a moderate inhibition (10% to 40%) was observed with group II compounds, strong inhibition of calcein efflux (over 100% comparing to the maximal inhibition of MK571) was observed with group III compounds [Fig 4]. The results suggest that the torsion angles (i.e. steric effect) between the biphenyl rings of the test compounds is the key factor of determining the interaction with ABCC2/MRP2. The compounds with the smallest ortho substitutions (hydrogen, fluorine and oxygen), thus the least torsions angle of the biphenyl (37^o – 45^o), are neither substrates nor inhibitors of ABCC2/MRP2 [Table 2]. The ABCC2/MRP2 transporter interaction increases as the steric bulk of the ortho substitution increases. When the 2-position is occupied by a methyl group, the torsion angle becomes moderate (54^o - 65^o) and the compound behaves as an ABCC2/MRP2 substrate, as well as a mild inhibitor (10-40%

inhibition of transport when compared to MK571). For the 2, 2'-dimethyl substituted biphenyls, the torsion angles are further increased (78^o – 87^o), and the strongest inhibition of ABCC2/MRP2 transport was observed [Table 2]. These results are in keeping with the report from van Zanden et al. in a study of a large number of flavonoids, that the inhibition of MRP1 is related to the dihedral angle between the phenyl and the chromenone core, which suggest that the steric effect is a critical factor for ABCC1/MRP1 inhibition (van Zanden et al., 2005).

Several inhibition mechanisms for ABCC/MRPs have been proposed in the literature. The inhibitory compounds might interfere with ABCC/MRPs through drug binding, ATP binding, ATP hydrolysis, drug transport, or ADP release (Boumendjel, 2003). ABCC2/MRP2 inhibitors, such as probenecid and azithromycin, are also transported by ABCC2/MRP2, which suggests that their inhibition may be through competition for drug-binding sites on the ABCC2/MRP2 (Chen et al., 2003; Sugie et al., 2004). The compounds from group II and III possess both an inhibitory and a transport interaction with ABCC2/MRP2, suggesting that the interactions between ABCC2/MRP2 and the biphenyl compounds occur at a drug binding site. Moreover, to further understand the transport kinetics for group II and III compounds, the concentration dependent transport in Caco-2 cells was investigated. As shown in Figure 5, the active efflux rate in Caco-2 cells increased with increasing concentrations of the test compound between 0.5-20 μM, but plateaued when the concentration exceeded 20 μM. The active efflux rate followed Michaelis-Menten kinetics with one-site binding model being the best fit:

$$V = \frac{V_{max}[S]}{K_m + [S]}$$

where V is the apparent linear initial rate, [S] the initial substrate concentration, V_{max} is the maximum transport rate, and K_m is the Michaelis-Menten constant. The estimated K_m for group II and III compounds transported by Caco-2 were 7.63 ± 1.07 and 9.13 ± 2.73 μM, respectively. There were no statistically significant differences in the K_m and V_{max} between the group II and group III compounds. These results suggest that the steric effect is more prominent on the inhibitory action than the transport activity of ABCC2/MRP2. This is consistent with a recent report (Hirono et al., 2005) that the steric effect contributes more (63%) than the electrostatic (33%) and lipophilicity (4%) effects on the ligand binding affinity to rat Abcc2/Mrp2. It was also reported that there are two electrostatically positive binding regions and two primary hydrophobic binding regions on the rat Abcc2/Mrp2. Sequence identity between the human and rat MRP2 is 72%. If the human ABCC2/MRP2 has the comparable binding pocket to rat ABCC2/MRP2, it is possible that the two branched polar groups, 3-carbamoyl and 4-urea on pyrazole, interact with the two primarily positive regions deep in the binding site, and the biphenyl ring interacts with the two hydrophobic binding regions. Further studies are needed to confirm whether the 4-(3-carbmoyl-4-urea)-pyrazole, which was kept constant in this study, is involved in the recognition of the ABCC2/MRP2 binding site.

In conclusion, for a series of tested biphenyl compounds, the interaction between ABCC2/MRP2 and the small molecules do not correlate with a variety of physicochemical properties. However, the ABCC2/MPR2 interactions do correlate with an increase in the steric bulkiness of ortho-substitutions, indicating that the steric interaction is the predominent factor for understanding ABCC2/MRP2 interactions in this study. These results could help define the

three-dimensional structural requirements of ABCC2/MRP2 interaction and provide SAR to support drug discovery.

Acknowledgement

We would like to thank Jing Wu, Lance Heinle, Susan Dudek for sample analysis. We are also grateful to Dr. Jeffrey Stevens and Dr. Archie Thurston for their helpful suggestions on our manuscript.

Reference

Artursson P, Palm K and Luthman K (2001) Caco-2 monolayers in experimental and theoretical predictions of drug transport. *Adv Drug Deliv Rev* **46:**27-43.

Asakura E, Nakayama H, Sugie M, Zhao YL, Nadai M, Kitaichi K, Shimizu A, Miyoshi M, Takagi K, Takagi K and Hasegawa T (2004) Azithromycin reverses anticancer drug resistance and modifies hepatobiliary excretion of doxorubicin in rats. *Eur J Pharmacol* **484:**333-339.

Borst P, Evers R, Kool M and Wijnholds J (2000) A family of drug transporters: the multidrug resistance-associated proteins. *J Natl Cancer Inst* **92:**1295-1302.

Boumendjel A (2003) Aurones: a subclass of flavones with promising biological potential. *Curr Med Chem* **10:**2621-2630.

Boumendjel A, Baubichon-Cortay H, Trompier D, Perrotton T and Di Pietro A (2005) Anticancer multidrug resistance mediated by MRP1: recent advances in the discovery of reversal agents. *Med Res Rev* **25:**453-472.

Chen C, Scott D, Hanson E, Franco J, Berryman E, Volberg M and Liu X (2003) Impact of Mrp2 on the biliary excretion and intestinal absorption of furosemide, probenecid, and methotrexate using Eisai hyperbilirubinemic rats. *Pharm Res* **20:**31-37.

Cui Y, Konig J, Buchholz JK, Spring H, Leier I and Keppler D (1999) Drug resistance and ATP-dependent conjugate transport mediated by the apical multidrug resistance protein, MRP2, permanently expressed in human and canine cells. *Mol Pharmacol* **55:**929-937.

Engman HA, Lennernas H, Taipalensuu J, Otter C, Leidvik B and Artursson P (2001) CYP3A4, CYP3A5, and MDR1 in human small and large intestinal cell lines suitable for drug transport studies. *J Pharm Sci* **90:**1736-1751.

Evers R, Kool M, van Deemter L, Janssen H, Calafat J, Oomen LC, Paulusma CC, Oude Elferink RP, Baas F, Schinkel AH and Borst P (1998) Drug export activity of the human canalicular multispecific organic anion transporter in polarized kidney MDCK cells expressing cMOAT (MRP2) cDNA. *J Clin Invest* **101:**1310-1319.

Fardel O, Jigorel E, Le Vee M and Payen L (2005) Physiological, pharmacological and clinical features of the multidrug resistance protein 2. *Biomed Pharmacother* **59:**104-114.

Gao J, Murase O, Schowen RL, Aube J and Borchardt RT (2001) A functional assay for quantitation of the apparent affinities of ligands of P-glycoprotein in Caco-2 cells. *Pharm Res* **18:**171-176.

Globisch C, Pajeva IK and Wiese M (2006) Structure-activity relationships of a series of tariquidar analogs as multidrug resistance modulators. *Bioorg Med Chem* **14:**1588-1598.

Gutmann H, Torok M, Fricker G, Huwyler J, Beglinger C and Drewe J (1999) Modulation of multidrug resistance protein expression in porcine brain capillary endothelial cells in vitro. *Drug Metab Dispos* **27:**937-941.

Hirohashi T, Suzuki H, Chu XY, Tamai I, Tsuji A and Sugiyama Y (2000) Function and expression of multidrug resistance-associated protein family in human colon adenocarcinoma cells (Caco-2). *J Pharmacol Exp Ther* **292:**265-270.

Hirono S, Nakagome I, Imai R, Maeda K, Kusuhara H and Sugiyama Y (2005) Estimation of the three-dimensional pharmacophore of ligands for rat multidrug-resistance-associated protein 2 using ligand-based drug design techniques. *Pharm Res* **22:**260-269.

Jedlitschky G, Leier I, Buchholz U, Hummel-Eisenbeiss J, Burchell B and Keppler D (1997) ATP-dependent transport of bilirubin glucuronides by the multidrug resistance protein MRP1 and its hepatocyte canalicular isoform MRP2. *Biochem J* **327 (Pt 1):**305-310.

Keppler D, Kamisako T, Leier I, Cui Y, Nies AT, Tsujii H and Konig J (2000) Localization, substrate specificity, and drug resistance conferred by conjugate export pumps of the MRP family. *Adv Enzyme Regul* **40:**339-349.

Keppler D and Konig J (2000) Hepatic secretion of conjugated drugs and endogenous substances. *Semin Liver Dis* **20:**265-272.

Kim KH (2001) 3D-QSAR analysis of 2,4,5- and 2,3,4,5-substituted imidazoles as potent and nontoxic modulators of P-glycoprotein mediated MDR. *Bioorg Med Chem* **9:**1517-1523.

Koike K, Abe T, Hisano T, Kubo T, Wada M, Kohno K and Kuwano M (1996) Overexpression of multidrug resistance protein gene in human cancer cell lines selected for drug resistance to epipodophyllotoxins. *Jpn J Cancer Res* **87:**765-772.

Kruh GD and Belinsky MG (2003) The MRP family of drug efflux pumps. *Oncogene* **22:**7537-7552.

Kusuhara H and Sugiyama Y (2002) Role of transporters in the tissue-selective distribution and elimination of drugs: transporters in the liver, small intestine, brain and kidney. *J Control Release* **78:**43-54.

Labrie P, Maddaford SP, Fortin S, Rakhit S, Kotra LP and Gaudreault RC (2006) A comparative molecular field analysis (CoMFA) and comparative molecular similarity indices analysis (CoMSIA) of anthranilamide derivatives that are multidrug resistance modulators. *J Med Chem* **49:**7646-7660.

Lather V and Madan AK (2005) Topological model for the prediction of MRP1 inhibitory activity of pyrrolopyrimidines and templates derived from pyrrolopyrimidine. *Bioorg Med Chem Lett* **15:**4967-4972.

Legrand O, Simonin G, Perrot JY, Zittoun R and Marie JP (1998) Pgp and MRP activities using calcein-AM are prognostic factors in adult acute myeloid leukemia patients. *Blood* **91:**4480-4488.

Leier I, Hummel-Eisenbeiss J, Cui Y and Keppler D (2000) ATP-dependent para-aminohippurate transport by apical multidrug resistance protein MRP2. *Kidney Int* **57:**1636-1642.

Leier I, Jedlitschky G, Buchholz U, Center M, Cole SP, Deeley RG and Keppler D (1996) ATP-dependent glutathione disulphide transport mediated by the MRP gene-encoded conjugate export pump. *Biochem J* **314 (Pt 2):**433-437.

Letschert K, Komatsu M, Hummel-Eisenbeiss J and Keppler D (2005) Vectorial transport of the peptide CCK-8 by double-transfected MDCKII cells stably expressing the organic anion transporter OATP1B3 (OATP8) and the export pump ABCC2. *J Pharmacol Exp Ther* **313:**549-556.

Lipinski CA, Lombardo F, Dominy BW and Feeney PJ (2001) Experimental and computational approaches to estimate solubility and permeability in drug discovery and development settings. *Adv Drug Deliv Rev* **46:**3-26.

Madon J, Eckhardt U, Gerloff T, Stieger B and Meier PJ (1997) Functional expression of the rat liver canalicular isoform of the multidrug resistance-associated protein. *FEBS Lett* **406:**75-78.

Matsushima S, Maeda K, Kondo C, Hirano M, Sasaki M, Suzuki H and Sugiyama Y (2005) Identification of the hepatic efflux transporters of organic anions using double transfected MDCKII cells expressing human OATP1B1/MRP2, OATP1B1/MDR1 and OATP1B1/BCRP. *J Pharmacol Exp Ther*.

Miller MD, Margot NA, Hertogs K, Larder B and Miller V (2001) Antiviral activity of tenofovir (PMPA) against nucleoside-resistant clinical HIV samples. *Nucleosides Nucleotides Nucleic Acids* **20:**1025-1028.

Nakagome I, Imai R, Hirono S, Maeda K, Kusuhara H and Sugiyama Y (2003) The three-dimensional quantitative structure-activity relationships of ligand molecules binding to the transporter, cMOAT/ MRP2. *Jap Pharm Ther* **31:**S143-S150.

Naruhashi K, Tamai I, Inoue N, Muraoka H, Sai Y, Suzuki N and Tsuji A (2002) Involvement of multidrug resistance-associated protein 2 in intestinal secretion of grepafloxacin in rats. *Antimicrob Agents Chemother* **46:**344-349.

Palm K, Stenberg P, Luthman K and Artursson P (1997) Polar molecular surface properties predict the intestinal absorption of drugs in humans. *Pharm Res* **14:**568-571.

Payen L, Courtois A, Campion JP, Guillouzo A and Fardel O (2000) Characterization and inhibition by a wide range of xenobiotics of organic anion excretion by primary human hepatocytes. *Biochem Pharmacol* **60:**1967-1975.

Prime-Chapman HM, Fearn RA, Cooper AE, Moore V and Hirst BH (2004) Differential multidrug resistance-associated protein 1 through 6 isoform expression and function in human intestinal epithelial Caco-2 cells. *J Pharmacol Exp Ther* **311:**476-484.

Raad I, Terreux R, Richomme P, Matera EL, Dumontet C, Raynaud J and Guilet D (2006) Structure-activity relationship of natural and synthetic coumarins inhibiting the multidrug transporter P-glycoprotein. *Bioorg Med Chem* **14:**6979-6987.

Rappa G, Lorico A, Flavell RA and Sartorelli AC (1997) Evidence that the multidrug resistance protein (MRP) functions as a co-transporter of glutathione and natural product toxins. *Cancer Res* **57:**5232-5237.

Robertson EE and Rankin GO (2006) Human renal organic anion transporters: characteristics and contributions to drug and drug metabolite excretion. *Pharmacol Ther* **109:**399-412.

Rost D, Mahner S, Sugiyama Y and Stremmel W (2002) Expression and localization of the multidrug resistance-associated protein 3 in rat small and large intestine. *Am J Physiol Gastrointest Liver Physiol* **282:**G720-726.

Sasaki M, Suzuki H, Ito K, Abe T and Sugiyama Y (2002) Transcellular transport of organic anions across a double-transfected Madin-Darby canine kidney II cell monolayer expressing both human organic anion-transporting polypeptide (OATP2/SLC21A6) and Multidrug resistance-associated protein 2 (MRP2/ABCC2). *J Biol Chem* **277:**6497-6503.

Schinkel AH and Jonker JW (2003) Mammalian drug efflux transporters of the ATP binding cassette (ABC) family: an overview. *Adv Drug Deliv Rev* **55:**3-29.

Shiozawa K, Oka M, Soda H, Yoshikawa M, Ikegami Y, Tsurutani J, Nakatomi K, Nakamura Y, Doi S, Kitazaki T, Mizuta Y, Murase K, Yoshida H, Ross DD and Kohno S (2004) Reversal of breast cancer resistance protein (BCRP/ABCG2)-mediated drug resistance by novobiocin, a coumermycin antibiotic. *Int J Cancer* **108:**146-151.

Sugie M, Asakura E, Zhao YL, Torita S, Nadai M, Baba K, Kitaichi K, Takagi K, Takagi K and Hasegawa T (2004) Possible involvement of the drug transporters P glycoprotein and multidrug resistance-associated protein Mrp2 in disposition of azithromycin. *Antimicrob Agents Chemother* **48:**809-814.

Suzuki H and Sugiyama Y (1998) Excretion of GSSG and glutathione conjugates mediated by MRP1 and cMOAT/MRP2. *Semin Liver Dis* **18:**359-376.

Taipalensuu J, Tornblom H, Lindberg G, Einarsson C, Sjoqvist F, Melhus H, Garberg P, Sjostrom B, Lundgren B and Artursson P (2001) Correlation of gene expression of ten drug efflux proteins of the ATP-binding cassette transporter family in normal human jejunum and in human intestinal epithelial Caco-2 cell monolayers. *J Pharmacol Exp Ther* **299:**164-170.

van Zanden JJ, Wortelboer HM, Bijlsma S, Punt A, Usta M, Bladeren PJ, Rietjens IM and Cnubben NH (2005) Quantitative structure activity relationship studies on the flavonoid mediated inhibition of multidrug resistance proteins 1 and 2. *Biochem Pharmacol* **69:**699-708.

Walle UK, Galijatovic A and Walle T (1999) Transport of the flavonoid chrysin and its conjugated metabolites by the human intestinal cell line Caco-2. *Biochem Pharmacol* **58:**431-438.

Wang EJ and Johnson WW (2003) The farnesyl protein transferase inhibitor lonafarnib (SCH66336) is an inhibitor of multidrug resistance proteins 1 and 2. *Chemotherapy* **49:**303-308.

Wang S, Folkes A, Chuckowree I, Cockcroft X, Sohal S, Miller W, Milton J, Wren SP, Vicker N, Depledge P, Scott J, Smith L, Jones H, Mistry P, Faint R, Thompson D and Cocks S (2004) Studies on pyrrolopyrimidines as selective inhibitors of multidrug-resistance-associated protein in multidrug resistance. *J Med Chem* **47:**1329-1338.

Yang CH, Chen YC and Kuo ML (2003) Novobiocin sensitizes BCRP/MXR/ABCP overexpressing topotecan-resistant human breast carcinoma cells to topotecan and mitoxantrone. *Anticancer Res* **23:**2519-2523.

FIGURE LEGENDS:

Figure 1. Correlation plots for inhibition of ABCC2/MRP2 mediated calcein efflux and the physicochemical properties of the test compounds. The inhibition of calcein efflux was measured in presence or absence of the test compounds (80 μM), compared to the inhibition of MK571 (25 μM). (A). Correlation with LogD at pH 7.4; (B). correlation with ClogP; (C). Correlation with number of hydrogen bond donors; (D). Correlation with topological polar surface area (tPSA).

Figure. 2. Correlation plots for Caco-2 efflux and the physicochemical properties of the test compounds. The efflux ratio of Caco-2 monolayer transport was calculated using basal to apical transport and apical to basal transport at concentration of 10 μM. (A). Correlation with LogD at pH 7.4; (B). Correlation with cLogP; (C). Correlation with number of hydrogen bond donors; (D). Correlation with topological polar surface Area (tPSA).

Figure 3. Illustration of torsion angles for a group of substituted bi-phenyl ring system. The torsion angles increase with increasing bulkiness of the substituents in the following order: H < F < OH < Cl < Me. The biphenyl ring systems are of the smallest torsion angles ($37^o – 45^o$) when they are unsubstituted or substituted with small atoms such as fluorine or oxygen. Chloride or 2-methyl substituted bi-phenyl ring systems exhibit moderate torsion angles (54^o - 65^o). The torsion angles of the 2, 2'-dimethyl substituted biphenyls are further increased ($78^o – 87^o$).

Figure 4. The correlation plots between torsion angles and the efflux in Caco-2 monolayer (A) or the inhibition of calcein efflux in MDCK gene transfected cells (B). Corresponding

to the increase of torsion angles between the biphenyl rings, the efflux ratio in Caco-2 monolayer increased, and so did the inhibition of calcein efflux. Based on the inhibition degree and the torsion angle range, the compounds were further classified into group I (37˚-45˚), group II (54^o - 65^o) and group III (78^o – 87^o).

Figure 5. Typical concentration-dependent transport of group II (A) and group III (B) compounds in Caco-2 monolayer. The apical to basolateral transport in Caco-2 cells followed Michaelis-Menten kinetics with one- site binding model being the best fit. The Michaelis-Menten constants (Km) were 7.63±1.07 and 9.13±2.73 μM in Group II and III compounds, respectively.

DMD Fast Forward. Published on March 19, 2007 as DOI: 10.1124/dmd.106.013250
This article has not been copyedited and formatted. The final version may differ from this version.

Table 1. Test compounds and their measured Caco-2 efflux with or without MRP2 specific inhibitor.

	IUPAC name	Structure	Caco-2 Efflux * (B→ A/A→B ratio)	Caco2 efflux with MK571 inhibition # (B→ A/A→B ratio)
1	2-chloro-4'-hydroxybiphenyl	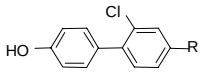	ND	N/A
2	4'-hydroxybiphenyl	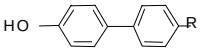	1.32	N/A
3	2-fluoro-4'-hydroxybiphenyl	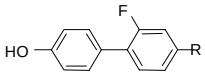	1.35	N/A
4	2-chloro-3'-fluoro-4'-hydroxybiphenyl	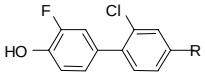	0.83	N/A
5	2-fluoro-4'-hydroxy-3'-methoxybiphenyl	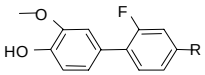	0.49	N/A
6	2-fluoro-4'-hydroxy-3',5'-dimethylbiphenyl	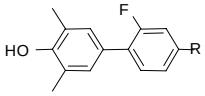	1.64	N/A
7	4'-hydroxy-3'-methoxybiphenyl	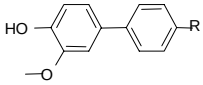	0.80	N/A
8	3'-fluoro-4'-hydroxybiphenyl	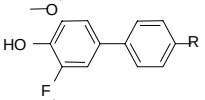	1.09	N/A
9	4'-hydroxy-3',5'-dimethylbiphenyl	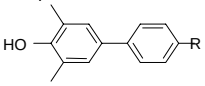	0.49	N/A
10	2-fluoro-4'-methoxy-3'-methylbiphenyl	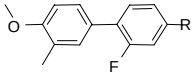	0.49	N/A
11	2-fluoro-4'-hydroxy-3'-methylbiphenyl	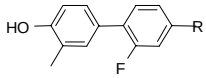	ND	N/A
12	3',4'-dihydroxybiphenyl	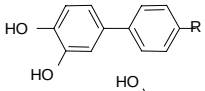	ND	N/A
13	3'-fluoro-2,4'-dihydroxybiphenyl	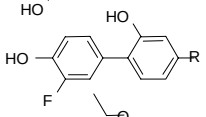	ND	N/A
14	2-ethoxy-3'-fluoro-4'-hydroxybiphenyl	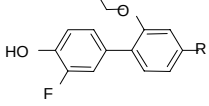	1.08	N/A

15	4'-hydroxy-2,3',5'-trimethylbiphenyl	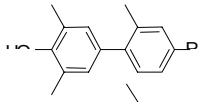	8.68	1.82
16	3'-fluoro-4'-hydroxy-2-methylbiphenyl	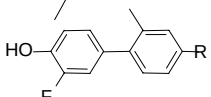	10.14	2.52
17	4'-hydroxy-2'-methylbiphenyl	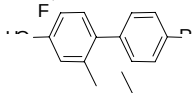	25.80	3.1
18	4'-hydroxy-2-methylbiphenyl	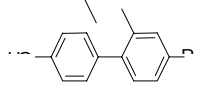	13.85	2.55
19	3'-bromo-4'-hydroxy-2,5'-dimethylbiphenyl	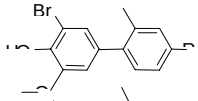	2.74	1.41
20	4'-hydroxy-3'-methoxy-2-methylbiphenyl	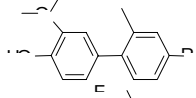	50.34	2.83
21	2',6'-difluoro-4'-hydroxy-2-methylbiphenyl	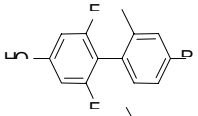	34.13	3.32
22	4'-methoxy-2,3'-dimethylbiphenyl	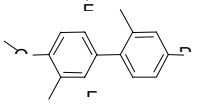	12.69	2.06
23	2',6'-difluoro-4'-methoxy-2-methylbiphenyl	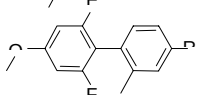	16.68	6.33
24	4'-hydroxy-2'-methyl-2-(trifluoromethyl) biphenyl	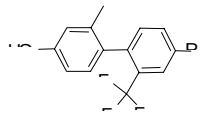	33.50	2.78
25	4'-hydroxy-2,2',3'-trimethylbiphenyl	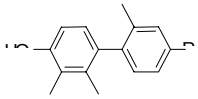	17.06	1.37
26	4'-hydroxy-2,2'-dimethylbiphenyl	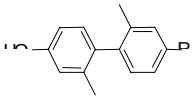	26.02	2.53

*, ND: Not detected; #, NA: Not applied

R = 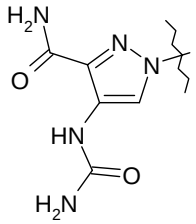

Table 2. Inhibition/transport profiles classified into three groups based on different torsion angles.

Group	Torsion Angles	Inhibition of Calcein efflux (% compared to MK571)	Caco-2 efflux (B→ A/A→B ratio >2)
I	40.1 ± 3.69	-1.7±3.6	No
II	55.6 ± 3.48*	18.9±8.1*	Yes
III	83.6 ± 4.88#	138.9±36.9#	Yes

*: Compared to Type I, P<0.01; #: compared to Group I and Group II, P<0.01

DMD Fast Forward. Published on March 19, 2007 as DOI: 10.1124/dmd.106.013250
This article has not been copyedited and formatted. The final version may differ from this version.

Figure 1

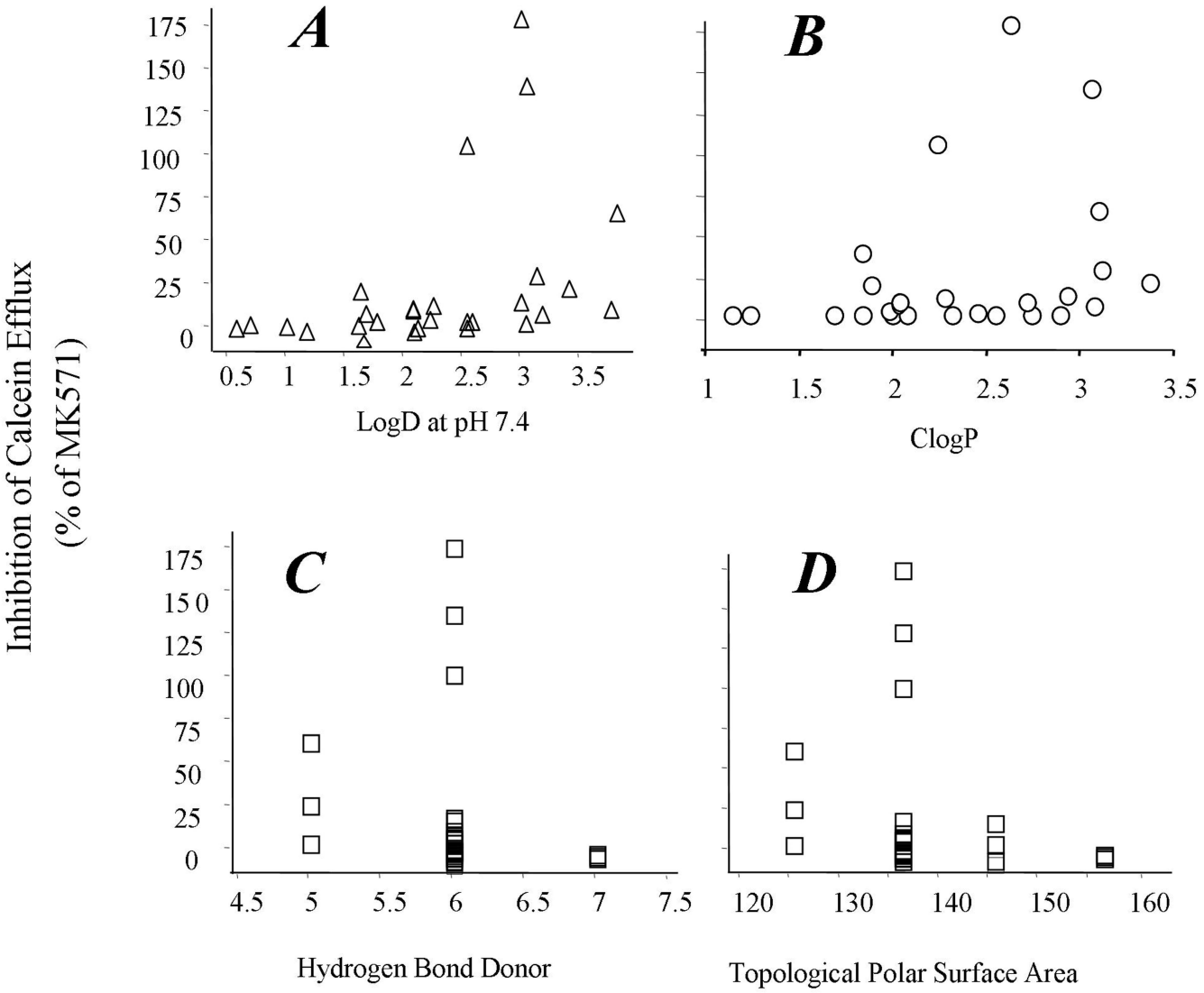

DMD Fast Forward. Published on March 19, 2007 as DOI: 10.1124/dmd.106.013250
This article has not been copyedited and formatted. The final version may differ from this version.

Figure 2

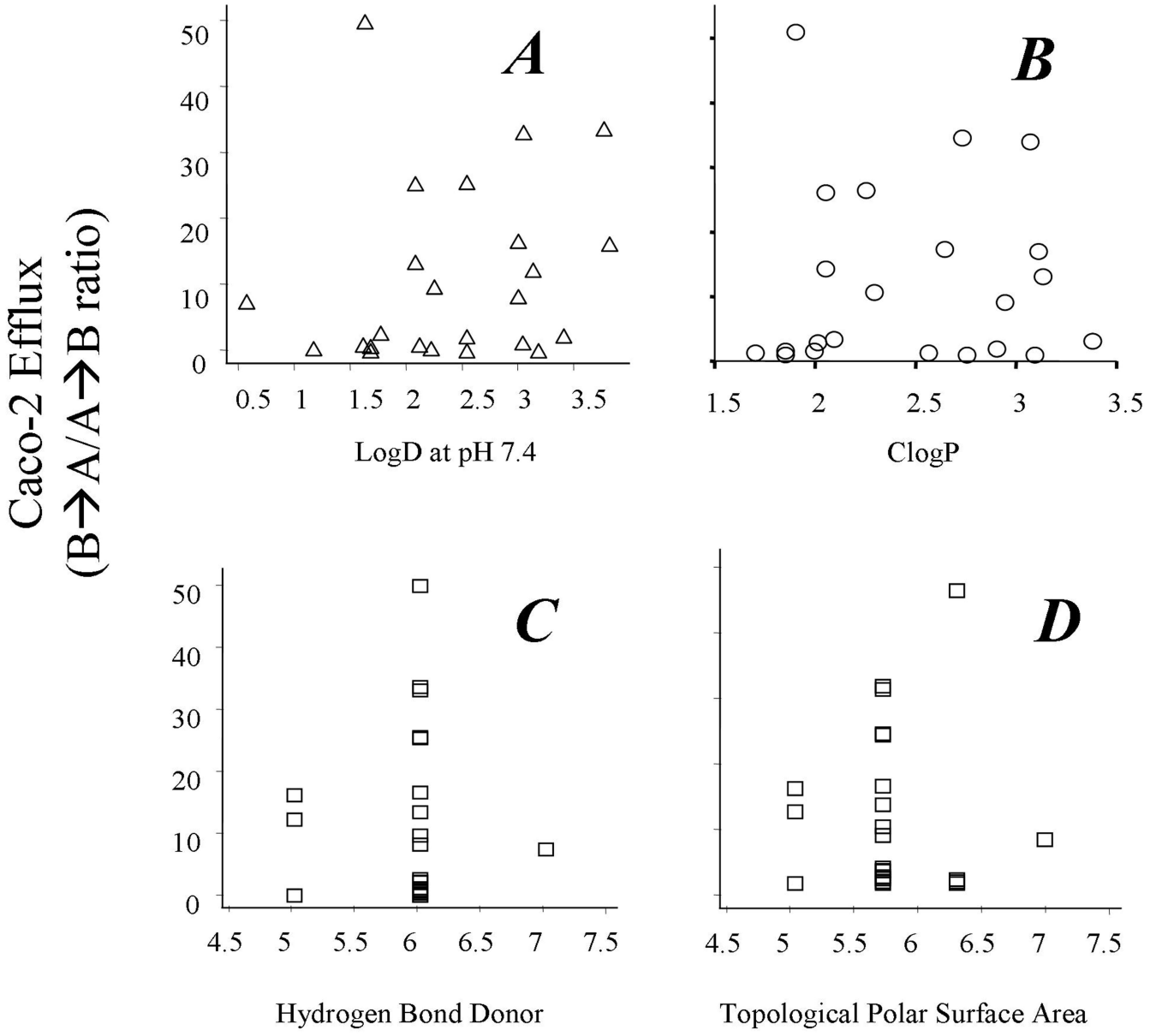

DMD Fast Forward. Published on March 19, 2007 as DOI: 10.1124/dmd.106.013250
This article has not been copyedited and formatted. The final version may differ from this version.

Figure 3

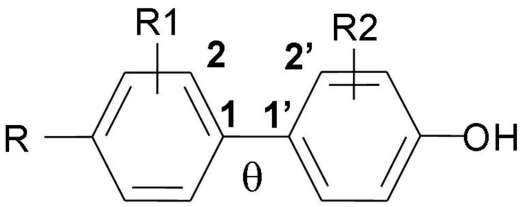

$\theta = (C_2, C_1, C_{1'}, C_{2'})$

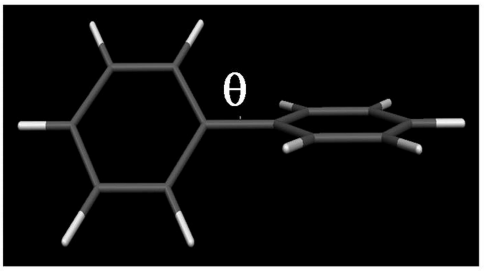

Substitution	Torsion Angle, θ
H	36.9
2'-F	39.0
2'-OH	43.0
2'-Cl	53.5
2'-Me	54.1
2'-Me, 2-Me	87.5
2'-CF3, 2-Me	85.1

DMD Fast Forward. Published on March 19, 2007 as DOI: 10.1124/dmd.106.013250
This article has not been copyedited and formatted. The final version may differ from this version.

Figure 4

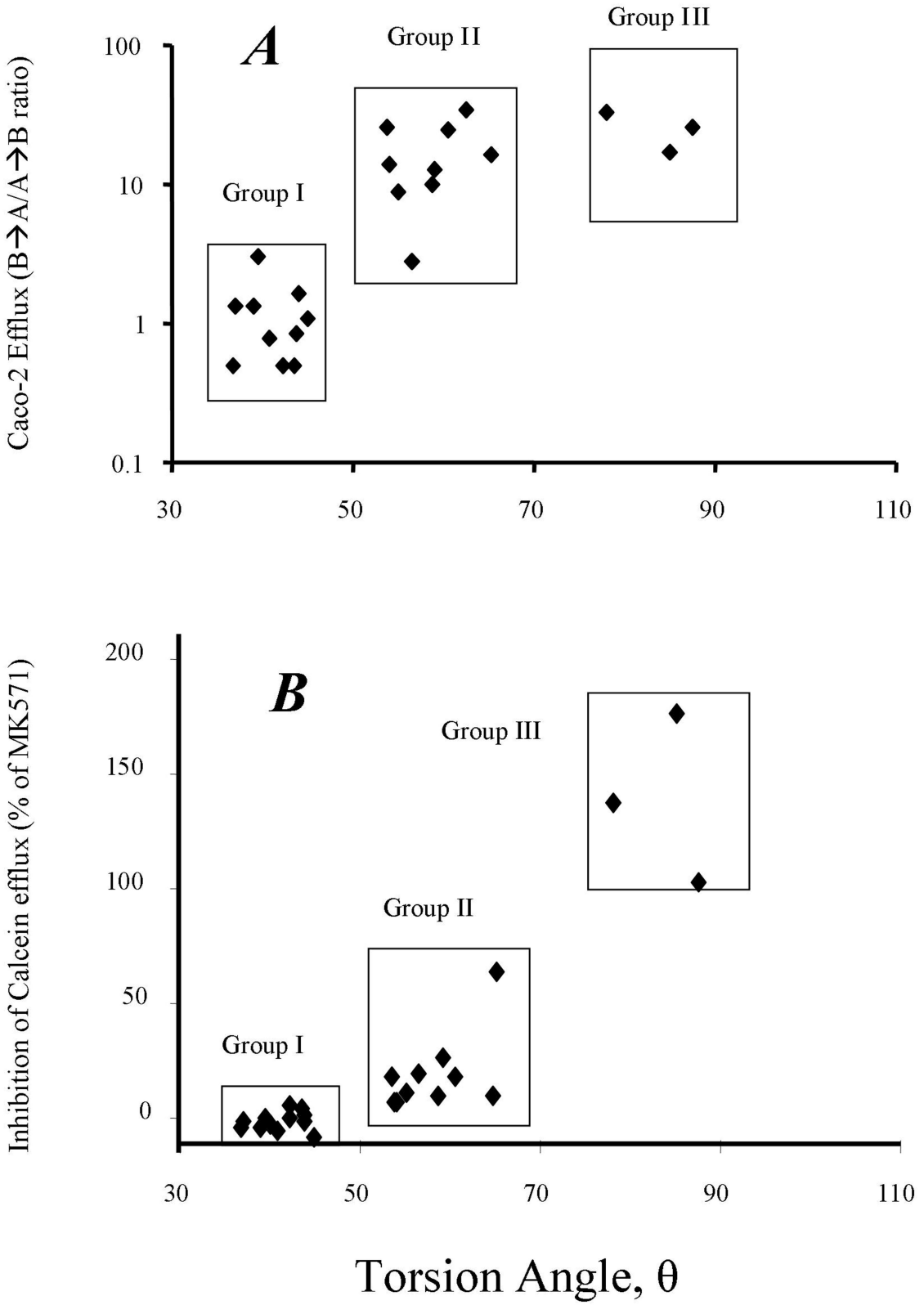

DMD Fast Forward. Published on March 19, 2007 as DOI: 10.1124/dmd.106.013250
This article has not been copyedited and formatted. The final version may differ from this version.

Figure 5